

Rational Design of a Light-Driven Molecular Switch Incorporating an Alizarin–Ru(bpy)₂ Fragment

Antonietta DelMedico, Scott S. Fielder, A. B. P. Lever, and William J. Pietro*

Department of Chemistry, York University, 4700 Keele Street, North York (Toronto), Ontario, Canada M3J 1P3

Received January 24, 1994[⊗]

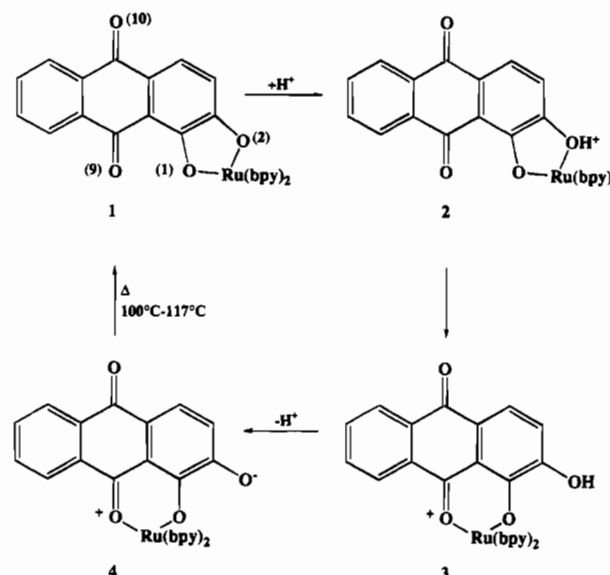
Ab initio and semiempirical AM1 studies are reported concerning the mechanism of a recently observed reversible acid-induced linkage isomerization in bis(bipyridine)(alizarin)ruthenium(II), where alizarin = 1,2-dihydroxy-9,10-anthraquinone. The calculations indicate that initial protonation occurs at the alizarin O(1), followed by a concerted proton shift to O(2) and 1,2 → 1,9 isomerization. The effects of protonation at various sites on the alizarin moiety on the metal to ligand bond orders and isomerization barriers are reported. The theoretically determined mechanism strongly suggests the possibility of utilizing the alizarin–Ru(bpy)₂ isomerization process as the basis for a novel reversible photodriven molecular switch. A prototypical molecular switch is discussed, and its switching mechanism and thermochemistry are investigated by further AM1 calculations.

Introduction

The field of molecular electronics is enjoying a slow but steady growth. Chemists are involved in this multidisciplinary field along primarily two avenues: the synthesis and study of new molecular components, such as molecular switches,¹ quantum dots and wires,² light antennas,³ redox polymers and oligomers,⁴ etc., and the development of methods for assembling these individual components into macromolecular systems capable of device or machine activity.⁵ Despite the enormously complex state of affairs involved in the latter endeavor, much progress have been made in just the last decade, and some very beautiful, albeit relatively simple, macromolecular electronic device assemblies, have emerged.⁶ It is still unclear what specific applications await the future of molecular electronics, but it is already crystal clear that chemistry will soon make revolutionary impact on the electronics industry.

Recently, we reported a novel switching phenomenon observed in an alizarin complex of Ru(bpy)₂²⁺, **1**.⁷ **1** is moderately

Scheme 1



stable in solution at high pH. However, lowering the pH below 5 results in linkage isomer **4**, presumably via the mechanism shown in Scheme 1. As the electronic absorption spectra of **1** and **4** are markedly different, we alluded to the possible utility of the complex as a type of molecular switch. We now report the results of theoretical studies concerning the mechanism in Scheme 1 and the possibility of creating light-addressable molecular switches based upon it.

Methods

All electronic structure calculations were performed at the semiempirical or *ab initio* levels as reported. Semiempirical AM1 calculations were performed using geometries fully optimized at the AM1 level. Geometries for *ab initio* calculations were AM1 preoptimized and then fully optimized at the HF/3-21G level. HF/6-31G* calculations were performed as single points using the 3-21G geometries. As AM1 is not yet parametrized for transition metals, the Ru(bpy)₂²⁺ fragment was modeled by a BF₂⁺ moiety to mimic its electron-withdrawing proper-

[⊗] Abstract published in *Advance ACS Abstracts*, February 15, 1995.

- (1) McCoy, C. H.; Wrighton, M. S. *Chem. Mater.* **1993**, *5*, 914.
- (2) Schmid, G. *Chem. Rev.* **1992**, *92*, 1709.
- (3) (a) Gust, D.; Moore, T. A.; Moore, A. L.; Devadoss, C.; Liddell, P. A.; Hermont, R.; Neiman, R. A.; Demanche, L. J.; DeGraziano, J. M.; Gouni, I. *J. Am. Chem. Soc.* **1992**, *114*, 3590. (b) Cogdell, R. G.; Frank, H. A. *Biochem. Biophys. Acta* **1987**, *895*, 63. (c) Gust, D.; Moore, T. A. *Adv. Photochem.* **1991**, *16*, 1. (d) Wasielewski, M. R.; Liddell, P. A.; Barrett, D.; Moore, T. A.; Gust, D. *Nature* **1986**, *322*, 570.
- (4) For recent reviews see: (a) Billingham, N. C.; Calvert, P. D. *Adv. Polym. Sci.* **1989**, *90*, 1. (b) Reynolds, J. R. *J. Mol. Electron.* **1986**, *2*, 1.
- (5) (a) Nogliki, H.; Pietro, W. J. *Chem. Mater.* **1994**, submitted. (b) Pietro, W. J. *Adv. Mater.* **1994**, *6*, 239. (c) Anderson, T. L.; Komplin, G. C.; Pietro, W. J. *J. Phys. Chem.* **1993**, *97*, 6577. (d) Ruiz-Hitzky, E. *Adv. Mater.* **1993**, *5*, 334. (e) Zhao, X. K.; Baral, S.; Fendler, J. H. *J. Phys. Chem.* **1990**, *94*, 2043. (f) Fendler, J. H. *CHEMTECH* **1985**, 686. (g) Fendler, J. H. *J. Macromol. Sci.—Chem.* **1990**, *A27*, 1167. (h) Fendler, J. H. *Chem. Rev.* **1987**, *87*, 877. (i) Kuhn, H. *J. Photochemistry* **1979**, *10*, 111. (j) Möbius, D. *Acc. Chem. Res.* **1981**, *14*, 63.
- (6) (a) Kuhn, H. *Molecular Electronics: Biosensors and Biocomputers*; Hong, F. T., Ed; Plenum Press: New York, 1989. (b) Inacker, O.; Kuhn, D.; Möbius, D.; Debuch, G. *Z. Phys. Chem. (Munich)* **1976**, *101*, 337. (c) Sugi, M.; Saito, M.; Fukui, T.; Iizima, S. *Thin Solid Films* **1983**, *99*, 17. (d) Baumann, U.; Lehmann, U.; Schwelbnuss, K.; van Boom, J. H.; Kuhn, H. *Eur. J. Biochem.* **1987**, *170*, 267. (e) Kuhn, H. *Phys. Rev. A* **1986**, *34*, 3409. (f) Carter, F. L., Ed. *Molecular Electronic Devices II*; Marcel Dekker: New York, 1987.

(7) DelMedico, A.; Dodsworth, E. S.; Auburn, P. R.; Lever, A. B. P.; Pietro, W. J. *Inorg. Chem.* **1994**, *33*, 1583.

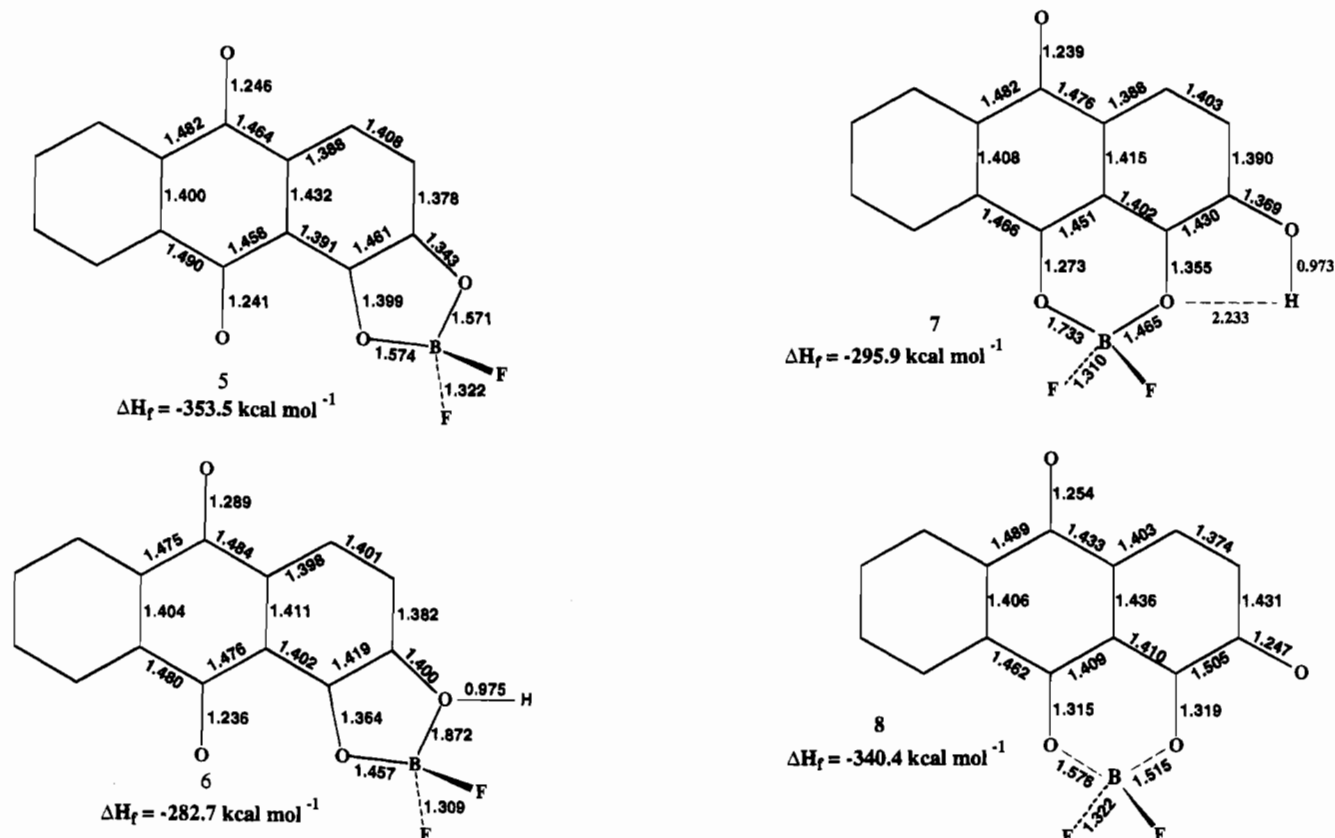


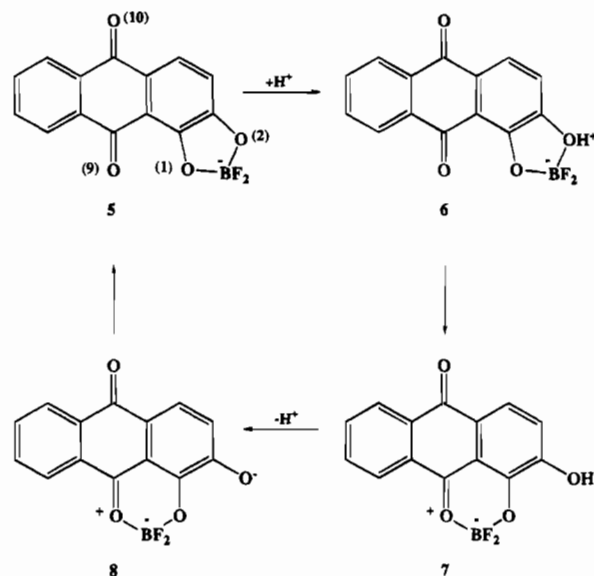
Figure 1. AM1 calculated geometries for species 5–8.

ties.⁸ Therefore, in the following study, Scheme 1 will be substituted by Scheme 2. Bond orders were calculated by the method of Lowdin⁹ using AM1 or HF/3-21G wave functions as indicated. Excited state energies and wave functions were calculated by the method of configuration interaction (CI) including the ground state and all single and double excitations involving the six highest occupied and eight lowest unoccupied molecular spin orbitals. CI calculations were performed as single points on the optimized ground state geometries. All ground state calculations and graphics were done using Spartan 2.0, and all excited state AM1 energies and wave functions were generated by the method of Stewart using in-house programs.¹⁰ Graphic images generated from excited state wave functions were displayed using in-house code. All calculations were performed on either a Silicon Graphics 4D/35, a Silicon Graphics R4000 ELAN, or an IBM 350 workstation.

Results and Discussion

The calculated AM1 geometries and heats of formation for isomers 5–8, are presented in Figure 1. The calculated thermochemistry is consistent with the mechanism proposed in Scheme 1 and modeled in Scheme 2. Structure 5 is calculated to be thermodynamically favored over isomer 8 by 13.1 kcal mol⁻¹, consistent with the observation that 1 is the predominant isomer formed during synthesis from Ru(bpy)Cl₂ and alizarin at high pH. In addition, complex 4 experimentally reverts back to 1 thermally, corroborating that the 1,2 isomer, 1, is indeed the more stable isomer. Upon protonation of 5 to form 6, the B–O(2) bond weakens considerably, as demonstrated by the unusually long bond distance (1.872 Å) and from the calculated bond order which decreases from 0.80 to 0.36 (Table 1).

Scheme 2

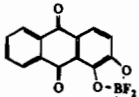
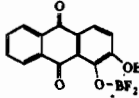
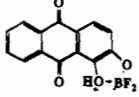
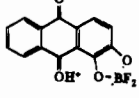
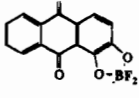


Protonated isomer 7 is calculated to be 13.2 kcal mol⁻¹ favored over 6, again consistent with the presumed mechanism in Scheme 1. Interestingly, the calculations show protonation of the keto oxygen O(10) to also significantly weaken the B–O(2) bond, as indicated by the B–O(2) optimized interatomic distance and bond order (Table 1). Inspection of the calculated geometry for 11 suggests a significant contribution from resonance form 11b.

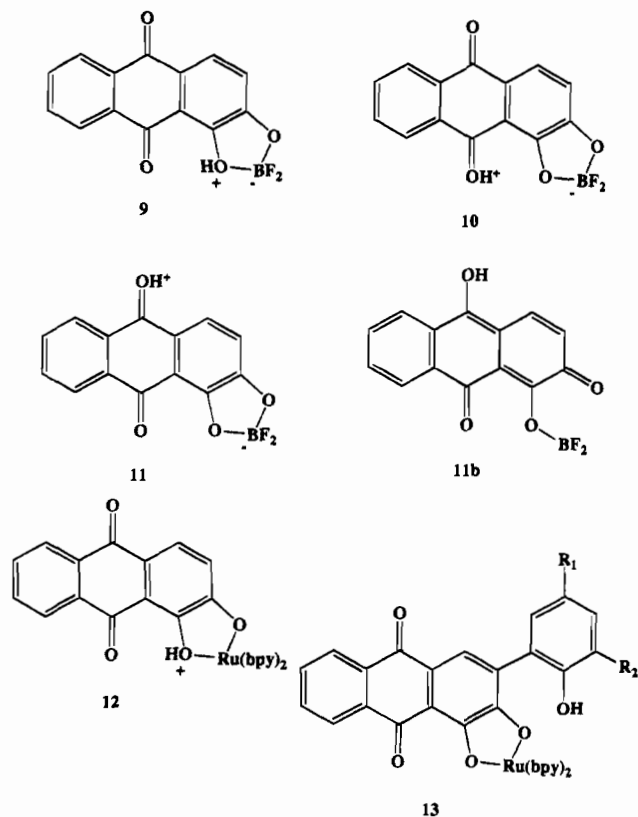
The barrier to rotation of the BF₂⁺ moiety about the C–O(1) bond was calculated for the direct conversion 5 → 8 and for 6 → 7 by incrementing the dihedral angle ϕ , indicated in Figure 2, while performing a full geometry optimization on the rest of the molecule. This was accomplished through the constrained

- (8) Metcalfe, R. A.; Dodsworth, E. S.; Lever, A. B. P.; Pietro, W. J.; Stufkens, D. J. *Inorg. Chem.* **1993**, *32*, 3581.
 (9) Hehre, W. J.; Radom, L.; Schleyer, P. v. R.; Pople, J. A. *Ab Initio Molecular Orbital Theory*; Wiley-Interscience: New York, 1986.
 (10) Armstrong, D. R.; Fortune, R.; Perkins, P. G.; Stewart, J. J. P. *J. Chem. Soc., Faraday Trans 2* **1972**, *68*, 1839.

Table 1. B-O(2) Bond Orders and Distances as a Function of Protonation at Various Sites

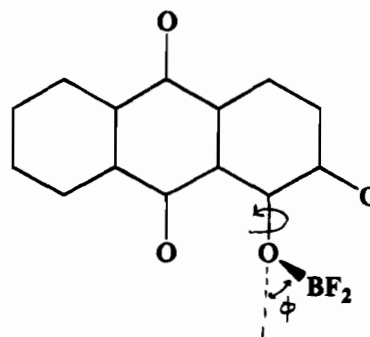
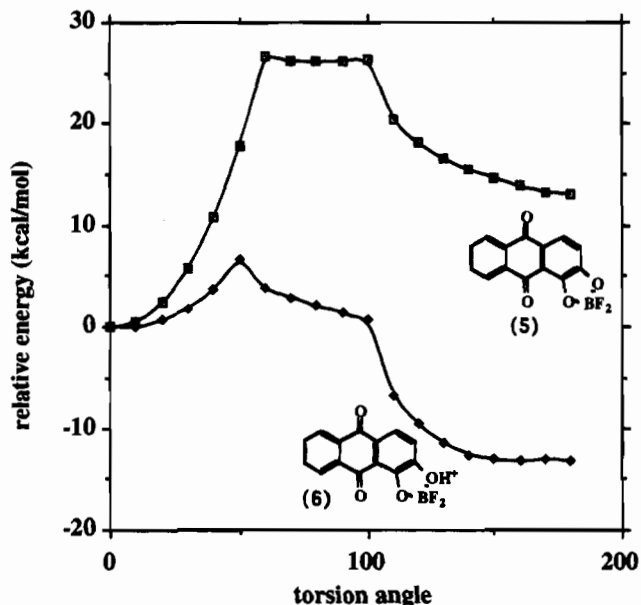
| Structure | B-O(2) bond | |
|---|-------------|------------|
| | r (Å) | Bond Order |
|  | 1.571 | 0.80 |
|  | 1.872 | 0.36 |
|  | 1.459 | 0.86 |
|  | 1.495 | 0.80 |
|  | 1.782 | 0.37 |

optimization method of Baker.¹¹ The AM1 heat of formation was plotted as a function of ϕ in Figure 3. The maximum in



the curve represents the barrier to rotation. Note the dramatic decrease (from 26.7 to 6.7 kcal mol⁻¹) in rotation barrier upon

(11) Baker, J. J. *Comput. Chem.* **1992**, *13*, 240.

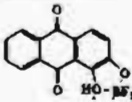
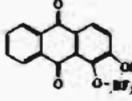
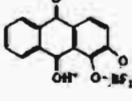
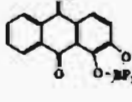
**Figure 2.** Constrained optimization for calculation of rotational barrier for species 5 → 8 and 6 → 7.**Figure 3.** AM1 calculated rotational barrier coordinate profile for 1,2 → 1,9 isomerization of species 5 and 6.

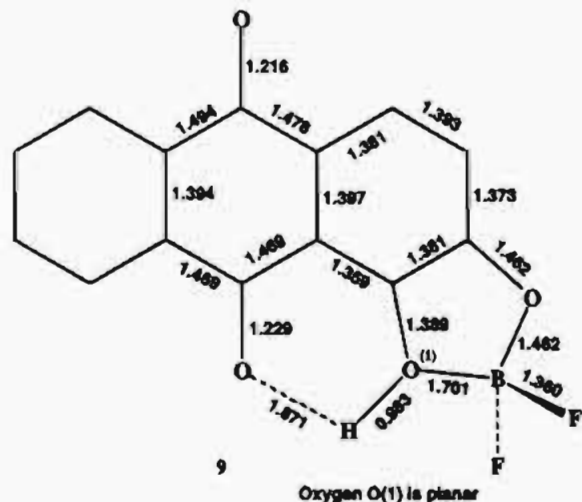
protonation of O(2). Note also the small absolute magnitude of the rotation barrier for 6 → 7. Solvation effects will tend to lower the barrier even further, potentially rendering the rotation thermally accessible.

The simple mechanism in Scheme 1 explains the experimental observations and is consistent with the calculated thermochemistry discussed above. However, further calculations suggest the mechanism to be somewhat more complicated in that the initial site of protonation is O(1), not O(2). Table 2 compares the relative AM1 heats of formation for 6 with structures 9–11, which correspond to the other three potential sites of protonation. The energy difference between 6 and 9 is calculated to be only 5.4 kcal mol⁻¹, and assigning the relative stabilities of tautomers based on such small energy differences may be misleading at the semiempirical level. We therefore reoptimized the geometries of 6–11 using *ab initio* HF/3-21G theory, and calculated single-point energies at the HF/6-31G* level. These data are also presented in Table 2, and confirm the semiempirical assignment that O(1) is the primary site of protonation of 1. The 3-21G structure of tautomer 9 (Figure 4) shows significant hydrogen-bonding interaction with keto oxygen O(9), which is doubtless responsible for the additional stabilization.

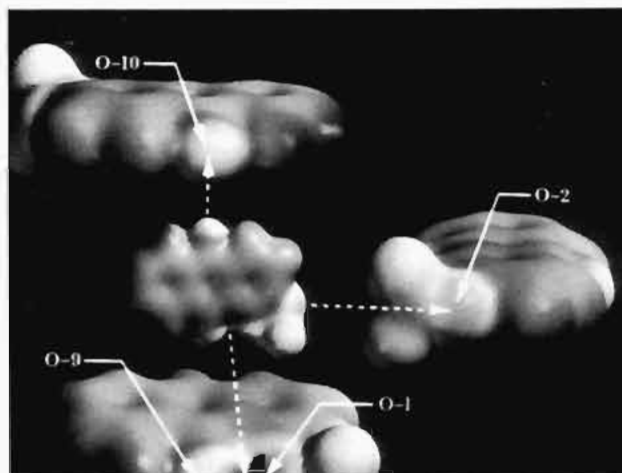
Further evidence for this assignment can be seen in the electrostatic potential function of 5 (Figure 5). The molecular electrostatic potential function (MEP) is defined by the interaction energy between a unit positive point charge and the molecule.¹² It is a continuous function defined at all loci about

Table 2. Calculated Relative Proton Affinities of Alizarin-BF₂ Oxygen Atoms

| Structure | $\Delta\Delta H_f$ (kcal mol ⁻¹) | | |
|---|--|----------|-----------|
| | AM1 | HF/3-21G | HF/6-31G* |
|  9 | 0 | 0 | 0 |
|  6 | 5.4 | 14.5 | 12.1 |
|  10 | 5.7 | 3.7 | 0.1 |
|  11 | 16.5 | 27.0 | 15.0 |

**Figure 4.** HF/3-21G optimized structure of tautomer 9.

a molecule. The MEP can be graphically displayed as an isosurface of fixed value or as a color-encrypted map on a surface of constant total electron density. Images of the latter type provide much useful information concerning relative proton affinities between molecules as well as at various sites within a molecule. Protons prefer to attack at regions of relatively high negative electrostatic potential, and direct relationships between a molecule's basicity and the magnitude of the MEP at the site of protonation have been observed.¹³ Figure 5 presents a gray-scale encrypted MEP mapped on the surface of 0.002 Å⁻³ for 5. This value for constant electron density was chosen as it closely approximates molecular size based on the atoms at their van der Waals radii.¹⁴ Both the MEP and density isosurface were generated from the HF/6-31G* wave function at the 3-21G optimized geometry. Regions of relatively high positive or negative electrostatic potential are indicated by a

**Figure 5.** HF/3-21G calculated molecular electrostatic potential (MEP) function of species 5 gray-scale encrypted on a surface of constant total electron density. Regions of relatively negative or positive MEP tend toward dark gray, while intermediate values tend toward white. The arrows indicate the locations of the oxygen atoms in the molecule.

dark gray coloration whereas intermediate values of the MEP are indicated by lighter shades of gray. The arrows indicate the location of the four oxygen atoms contained in this molecule. Here too oxygen O(1) is unambiguously assigned as the most likely site of protonation.

These results suggest two possible mechanisms for the formation of 3. One possibility is that at low pH protonation occurs predominantly at O(1), and to a small degree at O(2). Species 2 thus formed then converts to 3 by rotation about C-O(1). Since the concentration of 2 would be very low by direct protonation, conversion 2 → 3 must be a very rapid process. A second possibility is the rearrangement of isomer 12 directly to 3 via a concerted proton shift and linkage isomerization, with the driving force being the energy difference between the two isomers (18.6 kcal mol⁻¹). It is not likely that 12 first tautomerizes to 2 followed by isomerization, as this would require an initial process which is uphill by some 15 kcal mol⁻¹.

Light-Driven Switching Using the Alizarin-Ru(bpy)₂ Motif

The combined theoretical and experimental observations imply that protonation of 1 at site O(2) by any mechanism results in a very facile or even concerted rearrangement to 3. This leads to an interesting possibility concerning the fabrication of a light-driven molecular switch. It is well-known that the acidity of a phenolic compound is several orders of magnitude higher in its first excited single state (S₁) than in its ground state (S₀). This phenomenon is easily understood by looking at the molecular orbitals involved in the S₀ → S₁ transition in the phenol nucleus (Figure 6). The HOMO of phenol has considerable amplitude on oxygen, whereas the LUMO has very little. Promoting an electron from the HOMO to the LUMO (to form S₁) will result in a decrease in total electron density about the oxygen atom, increasing its effective electronegativity and further polarizing the O-H σ-bond. The result is a weaker O-H bond and, hence, greater acidity. This is also demonstrated, perhaps more directly, by observing changes in the MEP function upon excitation. The gas-phase acidity of phenols correlates well with the magnitude of the MEP at the site of

- (12) (a) Singh, U. C.; Kollman, P. A. *J. Comput. Chem.* 1984, 5, 129. (b) Davis, M. E.; McCammon, J. A. *J. Comput. Chem.* 1990, 11, 40.
 (13) The MEP has proven to be an exceptionally powerful method for identifying sites of protonation in organic molecules: Burke, L.; Fielder, S. S. Unpublished results.
 (14) Francl, M. M.; Hout, R. F., Jr.; Hehre, W. J. *J. Am. Chem. Soc.* 1984, 106, 563.

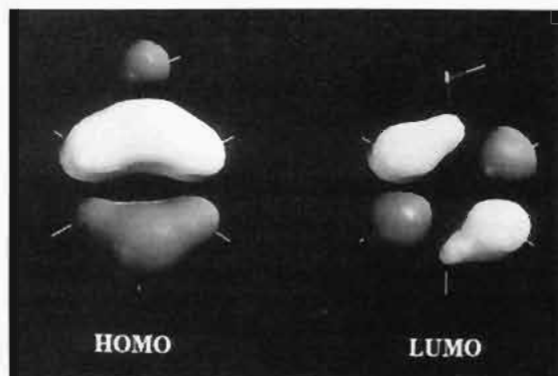


Figure 6. AM1 calculated HOMO and LUMO of phenol.

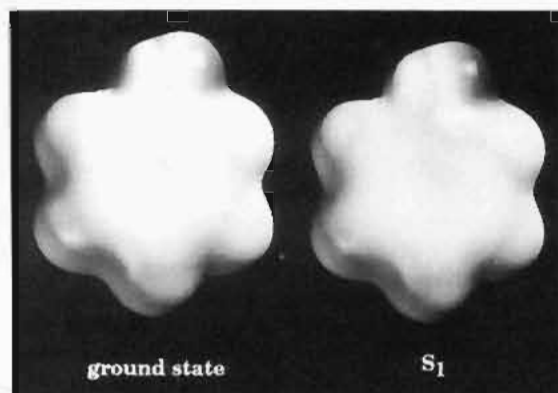
Figure 7. AM1-CI calculated molecular electrostatic potential (MEP) functions of phenol in (left) ground state and (right) S_1 , gray-scale encrypted on a surface of constant total electron density. Regions of relatively positive or negative MEP tend toward dark gray, while intermediate regions tend toward white.

Table 3. Acidity Constants of Substituted Phenols and Naphthols in Their Ground and First Excited States

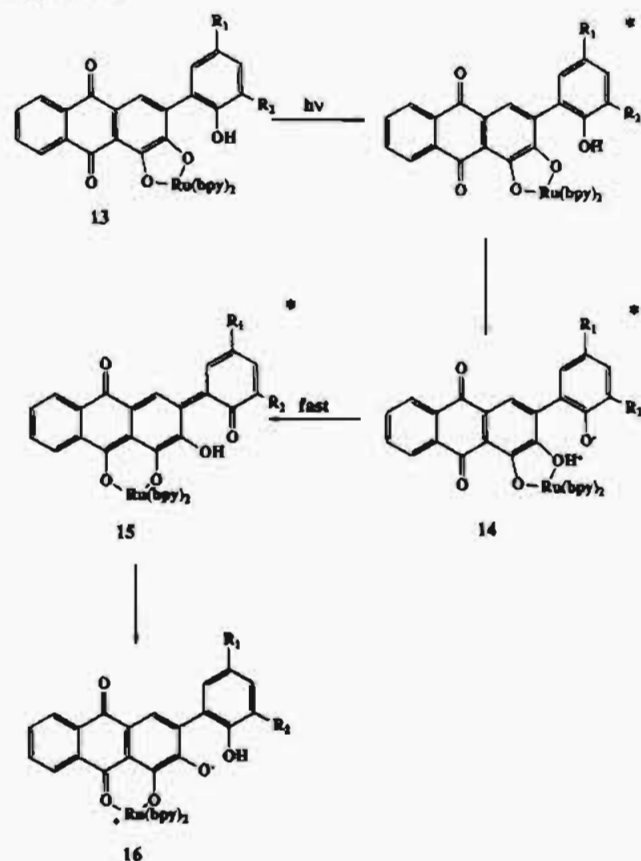
| system | $pK(S_0)$ | $pK(S_1)$ | ref |
|-------------------------|-----------|-----------|----------|
| <i>p</i> -cresol | 10.3 | 4.3 | <i>a</i> |
| <i>m</i> -cresol | 10.09 | 4.0 | <i>a</i> |
| <i>p</i> -bromophenol | 9.4 | 3.1 | <i>a</i> |
| <i>m</i> -methoxyphenol | 9.7 | 4.6 | <i>a</i> |
| 1-naphthol | 9.23 | 2.0 | <i>b</i> |
| 2-naphthol | 9.49 | 2.81 | <i>b</i> |
| 2-naphthol-5-sulfonate | 9.18 | 0.53 | <i>c</i> |
| 2-naphthol-6-sulfonate | 9.10 | 1.6 | <i>b</i> |
| phenol | 10.0 | 4.0 | <i>a</i> |
| <i>p</i> -fluorophenol | 9.21 | 3.8 | <i>a</i> |

^a Bartok, W.; Hartman, R. B.; Lucchesi, P. J. *Photochem. Photobiol.* **1965**, *4*, 499. ^b Weller, A. Z. *Phys. Chem.* **1958**, *17*, 224. ^c Weller, A. Z. *Phys. Chem.* **1952**, *56*, 662.

the acidic proton; the more positive the MEP, the more acidic the proton.¹³ Figure 7 presents the gray-scale encrypted MEP maps for S_0 and S_1 phenol, generated from AM1 CI calculations. These images predict an increase in acidity when phenol is excited to S_1 , and this is indeed observed. This is also observed in substituted phenols and naphthols, as presented in Table 3.

One can thus conceive of a novel light-addressable switching element for potential use in molecular electronic devices by tethering a phenolic moiety onto the alizarin– $Ru(bpy)_2$ complex as in **13**. The phenolic residue becomes strongly acidic when photoexcited, inducing an intramolecular proton transfer to tautomer **14***. **14*** then undergoes facile linkage isomerization to **15***, which subsequently transfers the proton back to the phenolic residue upon relaxation to the ground state, **16**. The net result is a light-triggered isomerization from **13** to **16**, summarized in Scheme 3. In order for this system to work, two restrictions must be placed on the acidity of the phenol

Scheme 3



group. First, its ground state pK_a must be high enough to prevent intramolecular proton transfer (to **14**) in the ground state. This puts a lower limit of ≈ 5 on the S_0 pK_a (based on the experimentally measured pK_b of **1**) for the phenolic moiety. Second, the S_1 pK_a of the phenol must be greater than ≈ 5 to enable proton transfer upon excitation. These criteria do not impose serious restrictions on our choice for the phenolic group, allowing a large number of substituted phenols (Table 3). One such example is the 2-(4-nitrophenyl) moiety. We therefore propose compound **17** to act as a light-addressable molecular switch.

Another criterion which must be met is that the excited state lifetime of the phenolic moiety must be long enough for intramolecular proton transfer to occur. This should almost certainly be the case since S_1 lifetimes of phenols are typically long (10^{-9} – 10^{-8} s) relative to tautomerization times ($\approx 10^{-12}$ s).¹⁵ Moreover, systems analogous to **17** are not without precedence.¹⁶

In order to further investigate the feasibility of the switching process in Scheme 3, AM1 calculations on the molecules involved with Scheme 3 were performed. Again the $Ru(bpy)_2^{2+}$ fragment was modeled by BF_2^+ (structure **18**). The AM1 optimized geometry of **18** is shown in Figure 8. Note the

(15) Brouwer, D. M.; MacLean, C.; Mackor, E. L. *Discuss. Faraday Soc.* **1965**, *34*, 121.

(16) (a) Catalán, J.; Fabero, F.; Claramunt, R. M.; Santa María, M. D.; de la Concepción Foces-Foces, M.; Caro, F. H.; Martínez-Ripoll, M.; Elguero, J.; Sastre, R. *J. Am. Chem. Soc.* **1992**, *114*, 5039. (b) Catalán, J.; Fabero, F.; Guifarro, M. S.; Claramunt, R. M.; Santa María, M. D.; de la Concepción Foces-Foces, M.; Caro, F. H.; Elguero, J.; Sastre, R. *J. Am. Chem. Soc.* **1990**, *112*, 747. (c) Catalán, J.; Fabero, F.; Guifarro, M. S.; Claramunt, R. M.; Santa María, M. D.; de la Concepción Foces-Foces, M.; Caro, F. H.; Elguero, J.; Sastre, R. *J. Am. Chem. Soc.* **1991**, *113*, 4046. (d) Catalán, J.; Pérez, P.; Fabero, F.; Wilshire, J. F. K.; Claramunt, R.; Elguero, J. *J. Am. Chem. Soc.* **1992**, *114*, 964.

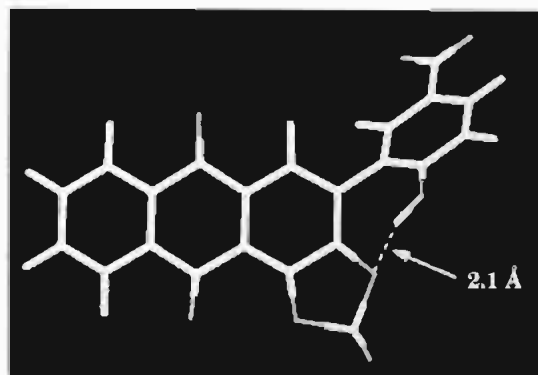


Figure 8. AM1 calculated geometry of structure 18.

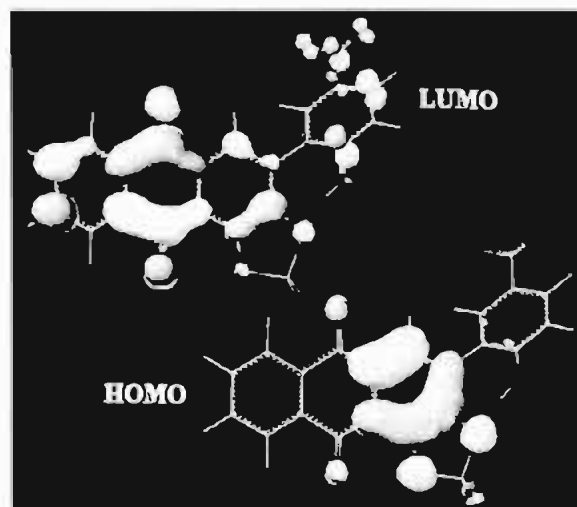


Figure 9. AM1 generated HOMO and LUMO of structure 18.

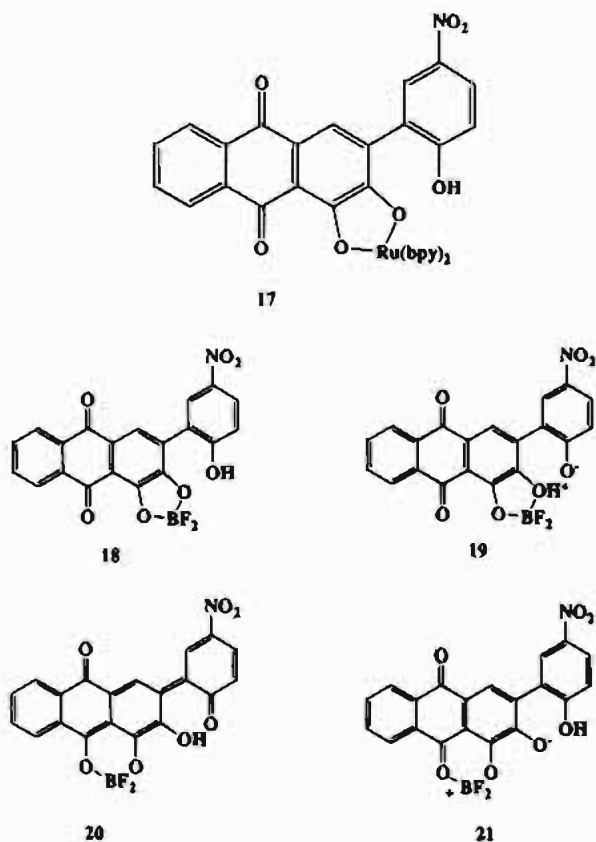
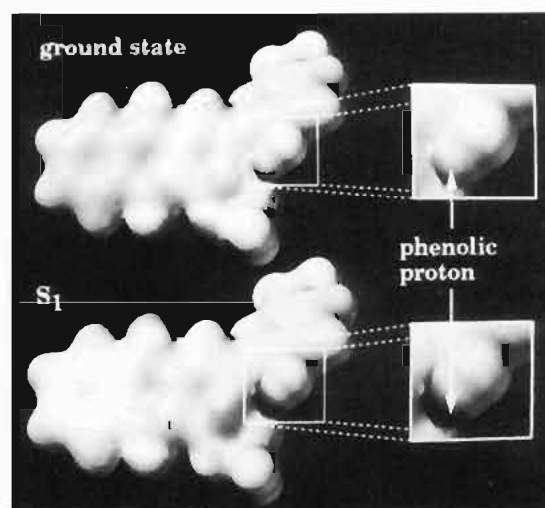


Table 4. Calculated Relative Tautomeric Stabilities of Model Molecular Switch Complex 18

| structure | ΔH_f° (AM1, kcal mol ⁻¹) | | $\lambda_{AM1}(nm)$ |
|-----------|---|----------------|---------------------|
| | S ₀ | S ₁ | |
| 18 | -377.2 | -276.2 | 276 |
| 19 | -361.8 | -295.8 | 488 |
| 20 | -363.9 | -312.1 | 521 |
| 21 | -366.0 | -284.4 | 336 |

Figure 10. AM1-CI calculated molecular electrostatic potential (MEP) functions of species 18 in (left) ground state and (right) S₁, gray-scale encrypted on a surface of constant total electron density. Regions of relatively positive or negative MEP tend toward dark gray, while intermediate regions tend toward white.

the rate of intramolecular proton transfer upon excitation. The AM1 heats of formation for species 18–21 in their S₀ and S₁ states are presented in Table 4. In the ground state 18 is the lowest energy isomer; proton transfer to 19 is uphill by 15.4 kcal mol⁻¹, and direct isomerization to 21 is uphill by 11.2 kcal mol⁻¹. The situation is quite different when the highest energy electron on the phenol is promoted to the LUMO (forming excited state S₁(ϕ)). AM1/CI predicts a 19.6 kcal mol⁻¹ driving force for proton transfer to 19* to occur, followed by an additional 16.3 kcal mol⁻¹ driving the isomerization to 20*. The system remains in tautomer 20* (the lowest energy isomer for S₁(ϕ)) until relaxation back to the ground state and then tautomerizes to 21.

The presence of the phenolic group actually enhances the

intramolecular hydrogen bond between the phenolic proton and O(2) of the alizarin, an interaction which should greatly facilitate

isomerization process **19** → **20** over the analogous isomerization in the unsubstituted alizarin complex, **6** → **7**. The LUMO of **18** is actually not localized on the nitrophenyl group but is located predominantly in the alizarin π -system (Figure 9). Excitation to S_1 is actually a phenol π to alizarin π^* charge transfer transition which enriches O(9) with π -electron density, making it a better nucleophile, and thus facilitating the isomerization. Note also that, as expected, the phenolic proton exhibits enhanced positive electrostatic potential in the excited state over the ground state, as revealed by the MEP maps in Figure 10.

Conclusion

Through *ab initio* Hartree–Fock and semiempirical AM1 studies we propose that the mechanism of an observed acid-induced isomerization in bis(bipyridine)(alizarin)ruthenium(II) proceeds via initial protonation of alizarin at O(1), followed by a concerted proton shift to O(2) and 1,2 → 1,9 ligand linkage isomerization. We have also demonstrated that protonation of

O(2) considerably weakens the M–O(2) bond in a model boronated alizarin complex and lowers the isomerization barrier significantly. These results strongly suggest that the alizarin–Ru(bpy)₂ moiety can form the basis of a photodriven molecular switch in which an intramolecular proton transfer occurs from a tethered phenol. AM1 calculations on such a system (**18**) indicate photoinduced intramolecular proton transfer to proceed with ca. 20 kcal mol⁻¹ driving force and subsequent isomerization to occur with an additional 16 kcal mol⁻¹. The switch is predicted to be reversible, with the 1,2 isomer favored in the ground state by 11 kcal mol⁻¹.

Acknowledgment. The authors wish to thank the Natural Sciences and Engineering Research Council of Canada (NSERC) for their support of this work. We also thank Johnson-Matthey for a loan of RuCl₃ and Dr. Elaine S. Dodsworth for useful discussions.

IC9400503